

10/11/90 (a)  
M.Y. R. 0

Conf. 9009309-3

SLAC-PUB--5395

DE91 005757

# A Study of the $a_0(980)$ Meson in Radiative $J/\psi$ Decays\*

William S. Lockman

Santa Cruz Institute for Particle Physics  
Santa Cruz, CA USA 95064

Representing the MARK III Collaboration<sup>†</sup> at the Stanford Linear Accelerator Center  
Stanford, CA USA 94309

## ABSTRACT

Using the decay sequence  $J/\psi \rightarrow \gamma X, X \rightarrow a_0^\pm(980)\pi^\mp, a_0^\pm(980) \rightarrow \eta\pi^\pm$ , where  $X$  is the  $f_1(1285)$  or  $\eta(1400)$ , the  $\eta\pi^+$  vs.  $\eta\pi^-$  Dalitz plot intensity distributions are fitted with a model containing a coupled-channel parametrization of the  $a_0(980)$ . Preliminary values for the spin of  $X$ , the mass and width of the  $a_0^\pm(980)$  to  $\eta\pi^\pm$ , and the ratio of  $a_0^\pm(980)$  coupling strengths,  $g_K^2/g_\eta^2$ , to  $\bar{K}^0 K^+$  and  $\eta\pi^+$  are determined. From this model, the predictions for the ratios of branching ratios  $r_X = B(X \rightarrow a_0(980)\pi^-) \cdot B(a_0(980) \rightarrow K\bar{K}) / B(X \rightarrow a_0^\pm(980)\pi^\mp) \cdot B(a_0^\pm(980) \rightarrow \eta\pi^\pm)$  are compared with those obtained from MARK III Partial Waves analyses of the decays  $J/\psi \rightarrow \gamma K^0 K^\pm \pi^\mp$  and  $J/\psi \rightarrow \gamma \eta\pi^+\pi^-$ .

## I. INTRODUCTION

The MARK III collaboration<sup>†</sup> has recently performed isobar model partial wave analyses (PWA) of the decays:

$$J/\psi \rightarrow \gamma K^0 K^\pm \pi^\mp \quad (1)$$

and

$$J/\psi \rightarrow \gamma \eta\pi^+\pi^- \quad (2)$$

The PWA intensities for both decays are shown in Fig. 1. Below 1.35  $\text{GeV}/c^2$ , the  $f_1(1285)$  is observed in the  $1^{++} a_0(980)\pi$  partial wave, as shown in Figs. 1(b) and 1(d) for channels (1)<sup>1</sup> and (2)<sup>2</sup>, respectively. A pseudoscalar state at  $\sim 1400$   $\text{MeV}/c^2$ , the  $\eta(1400)$ , is observed by both analyses to decay through  $a_0(980)$  (cf., Figs. 1(a) and 1(c)). To

determine whether the same pseudoscalar state is observed in both decays, a coupled-channel analysis is performed to determine the ratio  $g_K^2/g_\eta^2$  of  $a_0^\pm(980)$  coupling strengths to  $\bar{K}^0 K^+$  and  $\eta\pi^+$ . The ratio of branching ratios

$$r = \frac{B(X \rightarrow a_0(980)\pi^-) \cdot B(a_0(980) \rightarrow K\bar{K})}{B(X \rightarrow a_0^\pm(980)\pi^\mp) \cdot B(a_0^\pm(980) \rightarrow \eta\pi^\pm)} \quad (3)$$

for the decay of  $X$ , where  $X$  is either the  $f_1(1285)$  or  $\eta(1400)$ , can then be estimated by the coupled channel model and compared with that obtained by the partial wave analyses. The coupled channel predictions and PWA ratios are referred to as  $r_{cc}$  and  $r_{pwa}$ , respectively. The PWA product branching ratios are listed in Table I.

\*Work supported in part by Department of Energy contracts No. DE-AC03-76SF00515, No. DE-AC02-76ER01195, No. DE-AC02-87ER40318, No. DE-AC03-81ER40050, and No. DE-AM03-76SF00010, and by the National Science Foundation.

MASTER

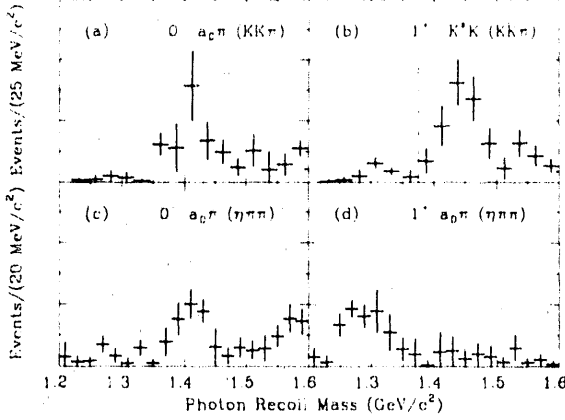


Fig. 1. (a-b):  $0^-+ a_0(980)\pi$  and  $1^{++} K^*K$  partial wave intensities for decay (1). The spin intensity to the left of the dashed line in 1(b) corresponds to  $1^{++} a_0(980)\pi$ . (c-d):  $0^-+ a_0(980)\pi$  and  $1^{++} a_0(980)\pi$  partial wave intensities for decay (2).

## II DATA

Events from decay (2) are observed in the  $\gamma\gamma\pi^+\pi^-$  final state. Events with  $\geq 3$  photons and two charged tracks with zero net charge are subjected to a four-constraint (4C) kinematic fit to the hypothesis  $\gamma\gamma\pi^+\pi^-$ . Candidate events with at least one  $\gamma\gamma$  combination within 70 MeV/ $c^2$  of the  $\eta$  mass and no combination within 35 MeV/ $c^2$  of the  $\pi^0$  mass are then 5C-fitted to the hypothesis  $\gamma\eta\pi^+\pi^-$ . The final sample is obtained by requiring that the 5C fit  $\chi^2$ -probability  $P(\chi^2) > 10\%$ , the energy of each photon  $E\gamma > 100$  MeV and that  $|\cos\gamma| < 0.95$ , where  $\gamma$  is the angle between the photon and the

$\eta$ -boost vector in the  $\eta$  rest frame. As shown in Fig. 2, clear  $a_0^\pm(980)$  signals are observed in both the  $1.22 < m_{\eta\pi\pi} < 1.35$  GeV/ $c^2$  and  $1.35 < m_{\eta\pi\pi} < 1.45$  GeV/ $c^2$   $\eta\pi^+\pi^-$  mass intervals (henceforth referred to as the “ $f_1(1285)$  region” and “ $\eta(1400)$  region”, respectively).

## III COUPLED CHANNEL MODEL

The observed Dalitz spectra shown in Figs. 2(a) and 2(d) are fitted with a model which describes the decay

$$X \rightarrow a_0^\pm(980)\pi^\mp, a_0^\pm(980) \rightarrow \eta\pi^\pm \quad (4)$$

From the measured four-vectors of the final state, the amplitude for this decay is constructed using an invariant tensor formalism.<sup>4,5</sup> The resulting symmetrized spin-one intensity is

$$I_1(m_+^2, m_-^2) = |\vec{p}_+ B W_+ + \vec{p}_- B W_-|^2 dLIPS \quad (5)$$

where  $m_+$  and  $\vec{p}_+$  ( $m_-$  and  $\vec{p}_-$ ) are the invariant mass and 3-momentum, respectively, of the  $\eta\pi^+$  ( $\eta\pi^-$ ) system and  $dLIPS$  is the Lorentz invariant phase space volume element.

For a spin-zero parent, the corresponding symmetrized intensity is

$$I_0(m_+^2, m_-^2) = \left| \frac{m_+^2 - m_\pi^2}{m_{\eta\pi\pi}^2} B W^+ + \frac{m_-^2 - m_\pi^2}{m_{\eta\pi\pi}^2} B W^- \right|^2 dLIPS \quad (6)$$

Table I.

MARK III  $a_0(980)\pi$  partial wave results

Decay sequence	$J_X^{PC}$	$M_X$ [MeV/ $c^2$ ]	$\Gamma_X$ [MeV]	Branching ratio [ $10^{-4}$ ]	Ref.
$J/\psi \rightarrow \gamma X, X \rightarrow a_0(980)\pi, a_0(980) \rightarrow K\bar{K}$	$0^-+$	$1416^{+8}_{-8} {}^{+7}_{-5}$	$54^{+37}_{-21} {}^{+13}_{-24}$	$6.6^{+1.7}_{-1.6} {}^{+2.4}_{-1.5}$	(1)
	$1^{++}$	1285	25	$0.66 \pm 0.26 \pm 0.29$	(3)
$J/\psi \rightarrow \gamma X, X \rightarrow a_0^\pm(980)\pi^\mp, a_0^\pm(980) \rightarrow \eta\pi^\pm$	$0^-+$	$1400 \pm 6$	$45 \pm 13$	$3.38 \pm 0.33 \pm 0.59$	(2)
	$1^{++}$	1285	25	$2.60 \pm 0.28 \pm 0.51$	(2)

The  $a_0^+(980)$  propagators  $BW^\pm$  are described by a modified version of the Flatté coupled channel model:<sup>6</sup>

$$BW^\pm \propto \frac{\sqrt{g_\eta^2}}{m_R^2 - m_\pm^2 - im_R(\Gamma_{\eta\pi^\pm} + \Gamma_{KK^\pm})} \quad (7)$$

where

$$\Gamma_{\eta\pi^\pm} = g_\eta^2 \frac{p_\eta}{m_\pm} \quad (8)$$

$$\Gamma_{KK^\pm} = \begin{cases} g_K^2 \frac{p_K}{m_\pm}, p_K^2 > 0 \\ ig_K^2 \frac{|p_K|}{m_\pm}, p_K^2 < 0 \end{cases} \quad (9)$$

where  $p_\eta$  ( $p_K$ ) is the momentum of the  $\eta$  ( $K$ ) in the  $\eta\pi$  ( $K\bar{K}$ ) rest frame and  $g_\eta^2$  ( $g_K^2$ ) is the coupling strength of the  $a_0^+(980)$  to the  $\eta\pi^\pm$  ( $K^0\bar{K}^\pm$ ) final state.

To account for events not described by the above amplitudes, an additional term,

$$I_{\text{back}} \propto dLIPS \quad (10)$$

is included in the fit. The fit is performed by minimizing the negative log likelihood<sup>7</sup>

$$-\sum_{k=1}^{\text{events}} \log \left\{ f \frac{I_k}{\int \epsilon dLIPS} + (1-f) \frac{1}{\int \epsilon dLIPS} \right\} \quad (11)$$

where  $\epsilon$  is the detection efficiency and  $I_k$  is the

spin-zero or spin-one intensity distribution, evaluated for the  $k^{\text{th}}$  event. The parameters determined from the fit are:  $f$ , the fraction of observed events attributed to the decay (4);  $m_R$ , the  $a_0(980)$  resonance mass; the  $a_0(980)$  width to  $\eta\pi^\pm$ ; and the coupling strength ratio,  $g_K^2 / g_\eta^2$ .

#### IV. RESULTS

The results of fitting the Dalitz plots in Figs. 2(a) and 2(d) are summarized in Table II. For each  $\eta\pi\pi$  mass interval, a comparison between alternate parent spin hypotheses is shown. For the  $f_1(1285)$  region, spin-one is favored by approximately 6 standard deviations, while the spin-zero hypothesis is favored in the  $\eta(1400)$  region by approximately  $7\sigma$ . For the fits with the smallest log likelihood,  $m_R$  and  $\Gamma_{\eta\pi}$  are in good agreement with values obtained by the LASS experiment.<sup>8</sup>

Since we are fitting only to the  $\eta\pi$  channel, the coupling ratio  $g_K^2 / g_\eta^2$  is rather poorly determined. A more precise measurement of this quantity is made by the LASS experiment who perform a simultaneous fit to their data and to those of Gay *et al.*<sup>9</sup> in both the  $\eta\pi$  and  $\bar{K}K$  channels. The coupling ratio obtained by the LASS experiment is

$$g_K^2 / g_\eta^2 = 2.4^{+1.1}_{-0.7} \quad (12)$$

Incorporating this value with its asymmetric error into our log likelihood fit yields the results shown in Table III.

Table II.

MARK III coupled channel fit results

fit interval:	$f_1(1285)$ region		$\eta(1400)$ region	
	$f$	$m_R$ (GeV/c <sup>2</sup> )	$f$	$m_R$ (GeV/c <sup>2</sup> )
parent spin:	0	0	0	0
$f$	$1.000 \pm 0.147$	$1.023 \pm 0.008$	$0.888 \pm 0.073$	$0.654 \pm 0.083$
$m_R$ (GeV/c <sup>2</sup> )	$0.105 \pm 0.018$	$0.105 \pm 0.018$	$1.001 \pm 0.007$	$1.004 \pm 0.010$
$\Gamma_{\eta\pi}$ (GeV)	$1.823 \pm 0.747$	$0.090 \pm 0.017$	$0.672 \pm 0.634$	$0.105 \pm 0.023$
$g_K^2 / g_\eta^2$				
Likelihood	-76.3	-94.1	-94.4	-70.3

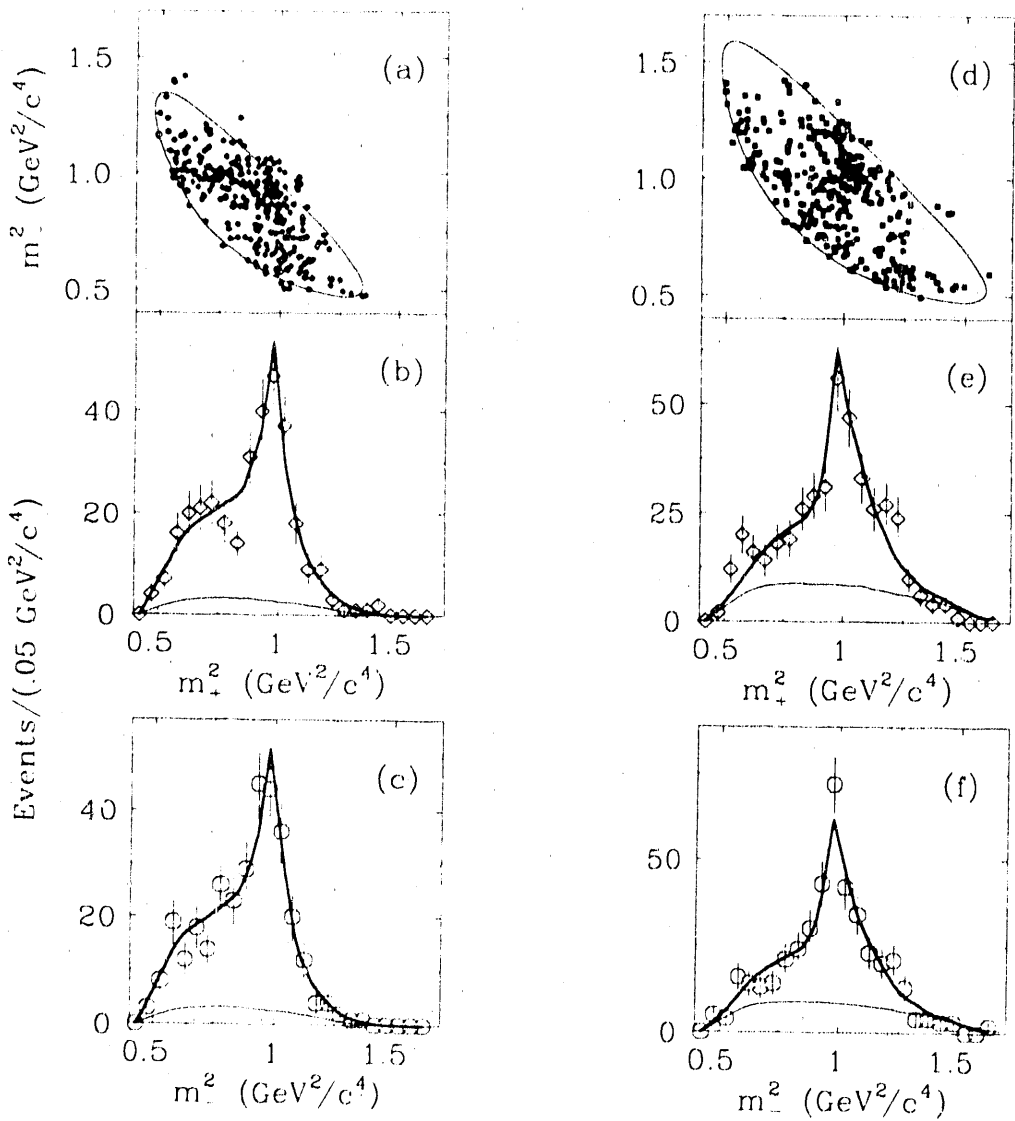


Fig. 2. Dalitz plots and projections corresponding to the  $f_1(1285)$  region, 2(a-c), and the  $\eta(1400)$  region(d-f). The Dalitz boundaries in 2(a) and 2(d) correspond to  $\eta\pi^+\pi^-$  masses of 1.283 and 1.400  $\text{GeV}/c^2$ , respectively. The heavy solid curves in 2(b-c) and 2(e-f) are the projections of the spin-one and spin-zero intensities, respectively, added to the background. The light curves represent the background intensities.

Table III.

MARK III coupled channel fit results incorporating the coupling constant ratio obtained by the LASS experiment.

fit interval:	$f_1(1285)$ region	$\eta(1400)$ region
parent spin:	1	0
$f$	$0.876 \pm 0.070$	$0.660 \pm 0.081$
$m_R$ (GeV/ $c^2$ )	$1.007 \pm 0.009$	$1.007 \pm 0.010$
$\Gamma_{\eta\pi}$ (GeV)	$0.097 \pm 0.021$	$0.102 \pm 0.022$
$g_K^2/g_\eta^2$	$1.631 \pm 0.584$	$1.944 \pm 0.553$
Likelihood	-92.6	-93.9

The relative errors on the coupling constant ratios are reduced; the values of the remaining parameters and log likelihoods do not change significantly.

Using the coupling ratios presented in Table III, the intensities in Eqs. (5) and (6) are numerically integrated over the  $f_1(1285)$  and  $\eta(1400)$  regions of  $\gamma\eta\pi^+\pi^-$  and  $\gamma K\bar{K}\pi$  phase space, respectively, to obtain the predicted ratios of branching ratios,  $r_{cc}$ . In Fig. 3, the dependence of  $r_{cc}$  on the coupling ratio is shown for the  $f_1(1285)$  and  $\eta(1400)$  mass intervals. In Table IV, these values are compared with those obtained from the PWA analyses of Reactions (1) and (2),  $r_{pwa}$ .

Table IV. ratio of branching ratio comparison

state X	$r_{cc}$	$r_{pwa}$
$f_1(1285)$	$0.25 \pm 0.09 \pm 0.05$	$0.25 \pm 0.10 \pm 0.16$
$\eta(1400)$	$0.69 \pm 0.20 \pm 0.14$	$1.95 \pm 0.54 \pm 0.74$

The first error associated with each entry is statistical, while the second error is systematic. The statistical errors on  $r_{cc}$  have been determined from the covariance matrix of the fitted parameters in Table III. The systematic errors have been estimated by (i) performing the fits in larger and

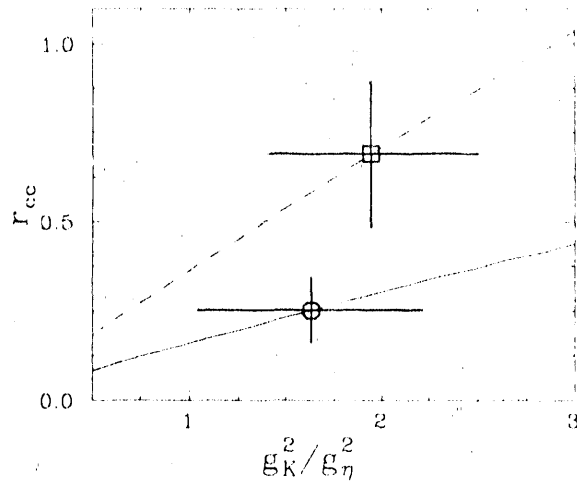


Fig. 3. The prediction,  $r_{cc}$ , plotted versus the coupling ratio, for the coupled channel fit results in the  $f_1(1285)$  region (solid curve) and in the  $\eta(1400)$  region (dashed curve). The open circle and open square correspond to the values obtained from the fit for the coupling ratio in the  $f_1(1285)$  and  $\eta(1400)$  regions, respectively. The error bars are statistical only.

smaller  $\eta\pi^+\pi^-$  mass intervals, (ii) imposing more restrictive criteria on the acceptance of the charged and neutral tracks and (iii) using a more elaborate coupled-channel parametrization.<sup>10,11</sup> In the  $f_1(1285)$  region, the agreement between  $r_{cc}$  and  $r_{pwa}$  is good. In this interval, only the  $a_0(980)\pi$  amplitudes are kinematically accessible, greatly reducing the uncertainties in the PWA results.

In the  $\eta(1400)$  interval,  $r_{pwa}$  appears to be larger than the coupled channel prediction, although the statistical and systematic uncertainties are large (both  $K^*K$  and  $a_0(980)\pi$  partial waves contribute to the  $K\bar{K}\pi$  width in this mass range). One possible explanation for the apparent discrepancy is that additional  $S$ -wave amplitudes, mistakenly identified as  $a_0(980)\pi$ , contribute to the  $K\bar{K}\pi$  structure at 1400 MeV/ $c^2$ . While this cannot be ruled out with the present statistics, a more likely explanation is that not all of the  $0^+a_0(980)\pi$  partial wave is resonant. Due to limited statistics and the

lack of a reference wave, the resonant component is difficult to estimate. However, the intensity distribution in Fig. 1(a) appears to contain a flat background. Refitting this distribution with an S-wave relativistic Breit-Wigner intensity and a flat background over the interval from 1.375 to 1.500  $\text{GeV}/c^2$  yields a branching ratio

$$B(J/\psi \rightarrow \gamma X, X \rightarrow a_0(980)\pi, a_0(980) \rightarrow K\bar{K}\pi) = (0.40 \pm 0.20^{+0.15}_{-0.09}) \times 10^{-3} \quad (13)$$

for the  $\eta(1400)$  state, and

$$r_{\text{PWA}} = 1.18 \pm 0.60^{+0.45}_{-0.41} \quad (14)$$

in agreement with the coupled channel prediction.

#### IV. SUMMARY AND CONCLUSIONS

The consistency of the MARK III partial wave analyses of reactions (1) and (2) has been examined through a preliminary coupled-channel analysis of  $a_0^\pm(980)$  decays to  $\eta\pi^\pm$ . In the  $f_1(1285)$  and  $\eta(1400)$  mass regions, the spin of the  $\eta\pi^+\pi^-$  is determined to be 1 and 0, respectively, in agreement with the PWA results for reaction (2). In the  $f_1(1285)$  region, the values obtained for the  $a_0(980)$  mass and  $\eta\pi$  width agree with those measured in the  $\eta(1400)$  region, and with values presented by the LASS experiment. The values obtained for  $g_K^2/g_\eta^2$  appear to be somewhat larger than the SU(3) value of 0.75,<sup>12</sup> assuming a pseudoscalar nonet mixing angle of  $-19.5^\circ$ . The ratio of  $f_1(1285)$  branching ratios determined by the coupled channel analysis agrees with that obtained by the PWA. In the case of the  $\eta(1400)$ , the two methods yield consistent results if 20-40% of the  $0^+ a_0(980)\pi$  signal is assumed to be nonresonant, as suggested by Fig. 1(a).

<sup>†</sup> Z. Bai, G. T. Blaylock, T. Bolton, J. C. Brient, T. Browder, J. S. Brown, K. O. Bunnell, M. Burchell, T. H. Burnett, R. E. Cassell, D. Coffman, V. Cook, D. H. Coward, F. DeJongh, D. E. Dorfan, J. Drinkard, G. P. Dubois, G. Eigen, K. F. Einsweiler, B. I. Eisenstein, T. Freese, C. Gatto, G. Gladding, C. Grab, J. Hauser, C. A. Heusch, D. G. Hitlin, J. M. Izen, P. C. Kim, J. Labs, A. Li, W. S. Lockman, U. Mallik, C. G. Matthews, A. I. Mincer, R. Mir, P. M. Mockett, B. Nemat, A. Odian, L. Parrish, R. Partridge, D. Pitman, S. A. Plaetzer, J. D. Richman, H. F. W. Sadrozinski, M. Scarlatella, T. L. Schalk, R. H. Schindler, A. Seiden, C. Simopoulos, I. E. Stockdale, W. Toki, B. Tripsas, F. Villa, M. Wang, S. Wasserbaech, A. J. Weinstein, S. Weseler, H. J. Willutzki, D. Wisinski, W. J. Wisniewski, R. Xu, and Y. Zhu.  
<sup>1</sup> Z. Bai *et al.* Phys. Rev. Lett. **65**, 2507 (1990).  
<sup>2</sup> M. Burchell, this conference.  
<sup>3</sup> Z. Bai *et al.*, SLAC-PUB-5201, August, 1990.  
<sup>4</sup> C. Zemach, Phys. Rev. **140**, B97 (1965).  
<sup>5</sup> J. Drinkard, *A Study of the  $K\bar{K}\pi$  Final State in  $J/\psi$  Radiative Decays*, University of California Santa Cruz report SCIPP-90/04 (Ph. D. Thesis), March, 1990 (unpublished).  
<sup>6</sup> S. M. Flatté, Phys. Lett. **63B**, 224 (1976).  
<sup>7</sup> The resolution in  $m_i^2$  is  $\sim 10 \text{ MeV}^2/c^4$ , which is small compared to the measured width of the  $a_0(980)$  presented in Section IV. Thus, the resolution function is approximated by a  $\delta$ -function in the likelihood expression.  
<sup>8</sup> T. Bienz *Strangeonium Spectroscopy at 11  $\text{GeV}/c$  and Cerenkov Ring Imaging at the SLD*, SLAC report SLAC-0369 (Ph. D. Thesis), July, 1990 (unpublished).  
<sup>9</sup> J. B. Gay *et al.*, Phys. Lett. **63B**, 220 (1976).  
<sup>10</sup> N. A. Tornqvist, Ann. Phys. **123**, 1 (1979); M. Roos and N. A. Tornqvist, Z. Phys. **C5**, 205 (1980); N. A. Tornqvist, Acta Phys. Pol. **B16**, 503 (1985).  
<sup>11</sup> N. N. Achasov *et al.*, Sov. J. Nucl. Phys. **32**(4), 566 (1980).  
<sup>12</sup> W. Dunwoodie, private communication.

#### DISCLAIMER

This report was prepared as an account of work sponsored by an agency of the United States Government. Neither the United States Government nor any agency thereof, nor any of their employees, makes any warranty, express or implied, or assumes any legal liability or responsibility for the accuracy, completeness, or usefulness of any information, apparatus, product, or process disclosed, or represents that its use would not infringe privately owned rights. Reference herein to any specific commercial product, process, or service by trade name, trademark, manufacturer, or otherwise does not necessarily constitute or imply its endorsement, recommendation, or favoring by the United States Government or any agency thereof. The views and opinions of authors expressed herein do not necessarily state or reflect those of the United States Government or any agency thereof.

END

DATE FILMED

10/24/91

